Annealing study of Fe_2O_3 nanoparticles: Magnetic size effects and phase transformations

X. N. Xu[a], Y. Wolfus, A. Shaulov, and Y. Yeshurun[b]
Department of Physics, Bar-Ilan University, Ramat-Gan 52900, Israel

I. Felner and I. Nowik
Racah Institute of Physics, Hebrew University, Jerusalem 91904, Israel

Yu. Koltypin and A. Gedanken
Department of Chemistry, Bar-Ilan University, Ramat-Gan 52900, Israel

(Received 28 September 2001; accepted for publication 10 January 2002)

Sonochemically synthesized Fe_2O_3 nanoparticles were annealed in air or in vacuum while their magnetization was continuously recorded. Annealing in vacuum at temperatures T_a between 240 and 450 °C produced nanophases of γ-Fe_2O_3 with average particle size ranging from 4 to 14 nm, depending on T_a. Phase transformation into α-Fe_2O_3 occurred directly by annealing in air, or via an intermediate Fe_3O_4 phase by annealing in vacuum at temperatures higher than 450 °C. Mapping the correlation between the magnetic properties and the annealing conditions, enables control of the annealing process to obtain nanocrystals of γ-Fe_2O_3, α-Fe_2O_3, or Fe_3O_4 with different particle size and magnetic properties. © *2002 American Institute of Physics.* [DOI: 10.1063/1.1457544]

I. INTRODUCTION

Metal oxides are of interest to many scientific and technological disciplines.[1] In particular, nanostructures of these materials have attracted considerable interest as they exhibit materials properties that differ strongly from those of the bulk phases.[2–6] These particle size effects enable tailoring the materials to a wide range of applications, including magnetic ferrofluids, electronics and catalysis.[7,8] Of special interest are gamma ferric oxide (γ-Fe_2O_3) particles as they retain important position in magnetic storage media.[9,10]

In this article we report on results of annealing sonochemically synthesized γ-Fe_2O_3 nanocrystals in different conditions, focusing on two aspects: (1) changes in the particle size distribution, and the associated variations in magnetic properties of the material during the annealing process and (2) transformations of γ-Fe_2O_3 nanoparticles to other iron–oxide phases caused by annealing at different conditions. Our experiments show that crystallites of γ-Fe_2O_3 with different average particle size ranging from 4 to 14 nm can be obtained by controlled annealing in vacuum. We report on the continuous change in the magnetic properties of the material during this annealing process.

A well known characteristic of the iron–oxide system is the variety of possible interconversions between the different phases.[1,11] This has been widely investigated for large particles. Our experiments show unique transformation properties for nanosize particles of γ-Fe_2O_3 caused by annealing at different conditions (ambient, temperature and time). The identification of the various phases has been based on their color, magnetic properties and Mössbauer spectra. Mapping the correlation between the magnetic properties of the annealing products and the annealing conditions, enables control of the annealing process to obtain nanocrystals of α-Fe_2O_3, γ-Fe_2O_3 and Fe_3O_4 with different particle size and magnetic properties.

II. EXPERIMENT

High purity Fe_2O_3 nanoparticles were prepared by a sonochemical method;[12,13] Namely, a solution of $Fe(CO)_5$ in decalin was ultrasonically irradiated under 1.5 atm of air at 0 °C for 3 h using a Sonics and Materials VC-1500 ultrasound processor. The volume of the sonicated solution was 500 ml. At the end of the sonification the solid product was separated by centrifugation, and washed thoroughly with dry pentane. The typical amount of the as-prepared product was 2.5 g. The product had a brown color typical of γ-Fe_2O_3. As prepared and annealed samples were characterized by x-ray diffraction (XRD), transmission electron microscopy (TEM), and Mössbauer spectroscopy (MS). The ^{57}Fe MS were measured with a 50 mCi^{57} Co:Rh source, using a constant acceleration mode. The isomer shift values are relative to Fe metals at room temperature. Magnetic properties of the samples were recorded in a vibrating sample magnetometer (Oxford 3001). Magnetic hysteresis loops were measured by applying a maximum magnetic field of 1.6 T. The saturation magnetization was obtained from magnetization versus $1/H$ curves, by extrapolating to $1/H=0$. TEM images were utilized to measure the particle size distribution and the average particle size, defined as $D=\langle dw\rangle/\langle w\rangle=\langle dV\rangle/\langle V\rangle=\langle d^4\rangle/\langle d^3\rangle$, where d, w and V are particle size, weight and volume, respectively. Differential scanning calorimetry (DSC) (Mettler DSC 25) at 10 °C/min was used to characterize the crystallization behavior of the material. Annealing experiments were performed in either air or vacuum maintained by a rotation pump.

[a]Permanent address: Physics Department, Nanjing University, Nanjing 210093, China.
[b]Electronic mail: yeshurun@mail.biu.ac.il

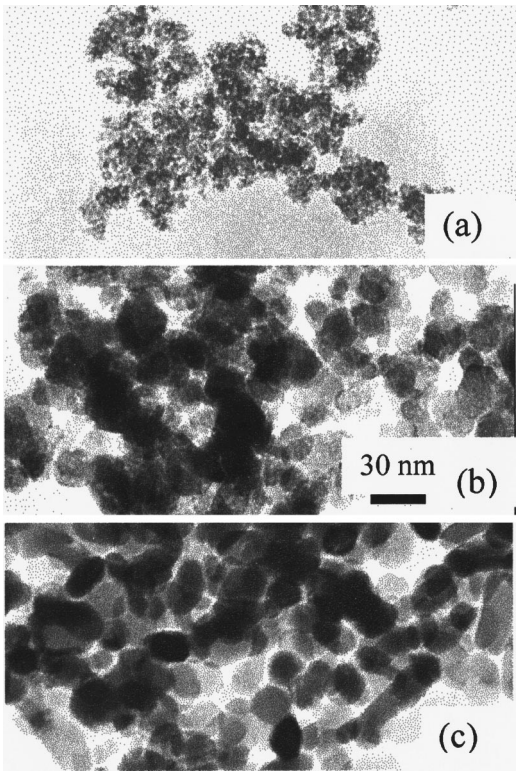

FIG. 1. RT TEM pictures of: (a) as prepared Fe_2O_3, (b) γ-Fe_2O_3 obtained after annealing in vacuum at 400 °C for 6 h, and (c) α-Fe_2O_3 obtained after sweeping temperature to 570 °C in air.

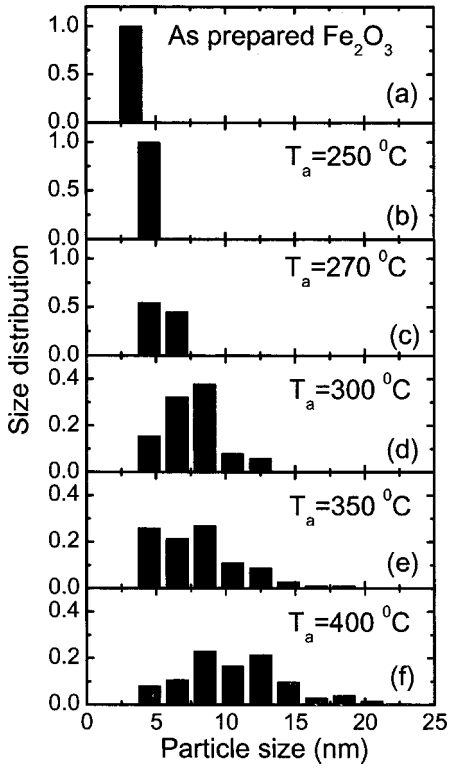

FIG. 2. Size distributions of Fe_2O_3 nanoparticles: (a) as-prepared sample, (b)–(f) after annealing at T_a=250, 270, 300, 350, and 400 °C.

III. CHARACTERIZATION OF AS-PREPARED SAMPLES

Figure 1(a) exhibits a TEM image of the as-prepared material, indicating an average particle size $D \sim 3$ nm with quite narrow particle size distribution [see Fig. 2(a)]. The smeared XRD peak shown in Fig. 3(a) is consistent with this value of D. Figure 3(b) shows the magnetization curve measured at room temperature (RT). As expected, it exhibits a superparamagnetic behavior, characteristic of small magnetic particles.[2–4] The magnetization curve is practically reversible with negligible coercive field $H_c = 0.5$ Oe and remanent magnetization $M_R = 5 \times 10^{-4}$ emu/g. DSC, Fig. 3(c), shows a smeared exothermic peak around 258 °C, with full width at half maximum from 160 to 310 °C, indicating an increase in the average size of the crystallites.

The RT Mössbauer spectrum, Fig. 4(a), consists of a broad doublet indicating the absence of a long range magnetic ordering. Computer analysis reveals the presence of two quadrupole doublets with the same isomer shift (IS) $= 0.46$ mm/s and linewidth of $W = 0.44(1)$ mm/s. The relative ratio of 4:1 corresponds to inequivalent Fe sites in the material. The quadrupole splitting (QS) are: $QS = eqQ/2 = 1.19(1)$ and $0.69(1)$ for the major and minor doublets, respectively. These values are typical of Fe^{+3} in the high spin state and are consistent with values obtained in Mössbauer spectra of Fe_2O_3 nanoparticles.[12,13]

IV. PARTICLE SIZE EFFECTS

As a result of annealing at elevated temperatures (above ~ 240 °C) the average particle size always increases and the particle size distribution widens. These changes may also be accompanied by a transformation into a different iron–oxide phase, such as α-Fe_2O_3 or Fe_3O_4 as described in Sec. V. In this section we report on annealing experiments in which the end product is always a γ-Fe_2O_3 nanophase with larger average particle size. This result has been obtained in vacuum annealing at temperatures from 240 to 450 °C for time periods from 2 to 6 h. During the annealing process, the magnetization of the samples was continuously recorded.

Figure 5(a) shows the isothermal normalized magnetization M/M_0 versus annealing time t_a at annealing temperatures T_a between 240 and 450 °C, in the presence of a magnetic field of 500 Oe. ($M_0 = 0.37$ emu/g is the RT magnetization of the as prepared sample). Evidently, the magnetization increases with the annealing time t_a until a stable saturation value m_s is reached. The annealing products were characterized at room temperature by magnetic hysteresis loop measurements, Mössbauer spectroscopy, and TEM.

The magnetization and the coercive field increase monotonically with annealing temperature as shown in Figs. 6(a) and 6(b). We ascribe this behavior to the increase in the average crystallite size of the γ-Fe_2O_3 nano-phase caused by the annealing. This claim has been confirmed by RT Mössbauer spectra of the final products and TEM measurements as described below.

Figures 4(b)–4(f) show the RT ^{57}Fe Mössbauer spectra measured after annealing at $250 \leqslant T_a \leqslant 400$ °C in vacuum. The main effect to be seen is the evolution of a doublet into a sextet through a series of complicated spectra composed of doublets and sextets. The doublet represents the fraction of small particles in which long range magnetic ordering is ab-

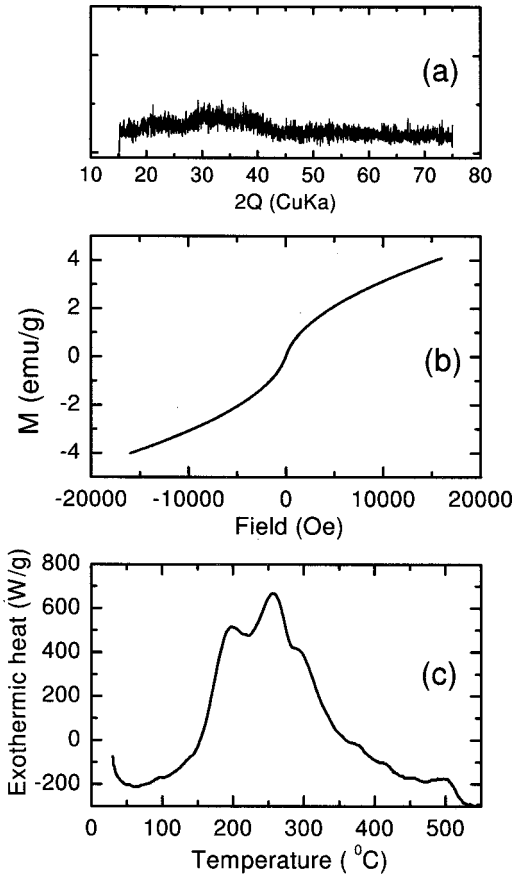

FIG. 3. (a) XRD pattern, (b) magnetization loop, and (c) DSC curve for as prepared Fe_2O_3.

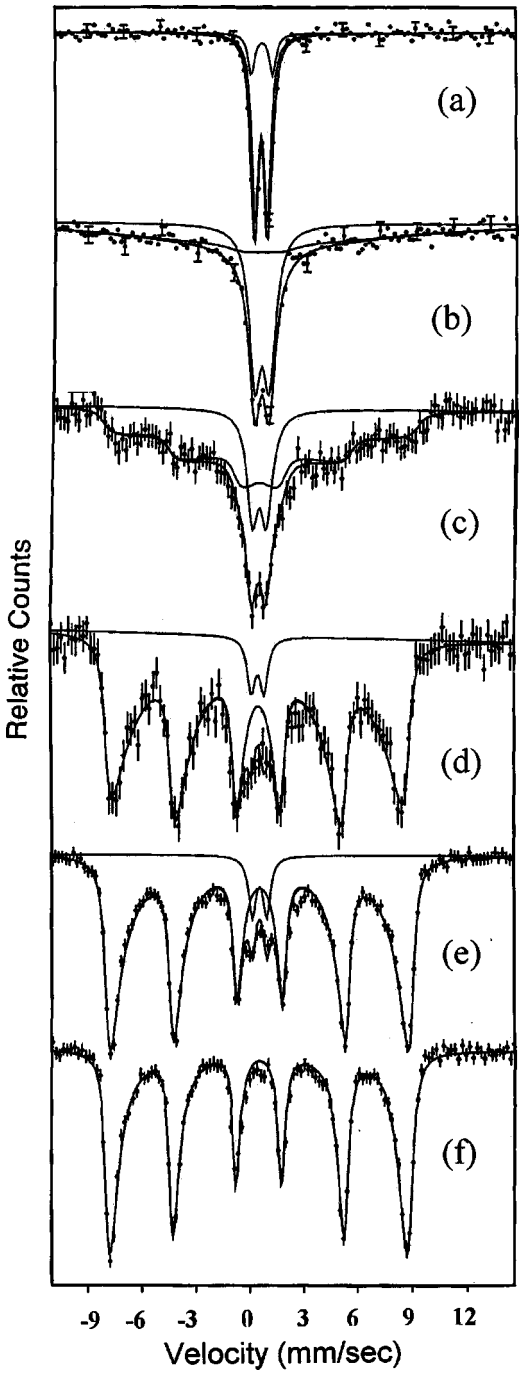

FIG. 4. RT MS of as prepared Fe_2O_3 (a), and its annealing products γ-Fe_2O_3 at various average size 4.5, 6, 9, 12, and 14 nm obtained at T_a = 250, 270, 300, 350, and 400 °C, from (b) to (f), respectively.

sent. The fraction of the sextet increases with the annealing temperature, indicating that more particles become magnetically ordered. A detailed analysis yields the sextet fraction of 37%, 77%, 93%, and 95% for $T_a = 250$, 270, 300, and 350 °C, respectively. TEM measurements indicate corresponding average particle size of about 4.5, 6, 9, and 12 nm, respectively. The data indicate that at 400 °C the fraction of the magnetically ordered material is close to 100%. This is consistent with the magnetic data described above. The Mössbauer spectrum measured after annealing at 400 °C (yielding 14 nm average particle size) consists of a pure sextet [see Fig. 4(f)]. Analysis of the sextet indicates a distribution of magnetic hyperfine fields due to the particle size distribution. The hyperfine parameters for this sextet are: a mean magnetic hyperfine field $H_{\text{eff}} = 52.0(5)T$, linewidth $W = 0.40$ mm/s, and IS = 0.48 mm/s. The sextet does not show a quadrupole effect. These parameters are consistent with the hyperfine values reported for bulk γ-Fe_2O_3 crystals.[1,14] We note that since the hyperfine field parameters for both α-Fe_2O_3 and γ-Fe_2O_3 are very close to each other, and the measured lines are quite broad, the Mössbauer spectrum is not sensitive enough to conclusively determine the magnetic phase obtained. However, the large magnetization value measured for these samples clearly indicates a γ-Fe_2O_3 phase.

The magnetization and Mössbauer measurements described above were complemented by particle size distribution measurements of the same samples after the completion of the annealing process. A typical TEM image of a sample annealed at $T_a = 400$ °C is shown in Fig. 1(b). The TEM images reflect roughly spherical nanoparticles with different size distribution depicted in Figs. 2(b)–2(f). Figure 6(c) shows the average particle size versus annealing temperature. As the annealing temperature increases from 250 to 400 °C the average particle size increases from 4.5 to 14 nm. The increase of the average particle size is accompanied by broadening of the particle size distribution as shown in Figs. 2(b)–2(f).

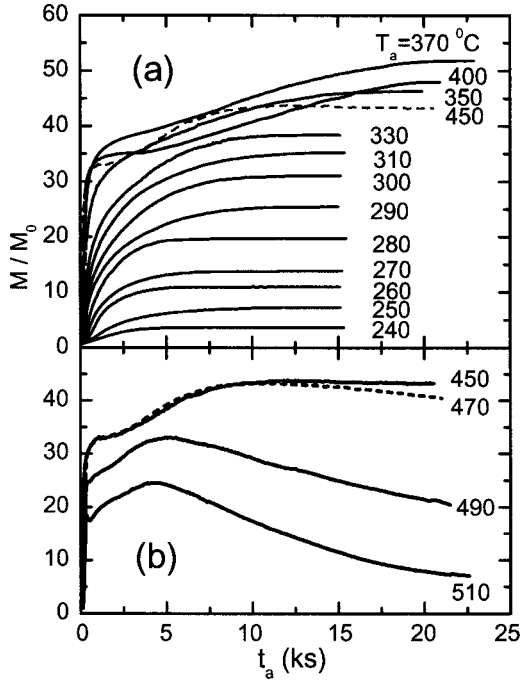

FIG. 5. Isothermal normalized magnetization vs annealing time at: (a) 240 °C$\leqslant T_a \leqslant$450 °C, and (b) for $T_a >$450 °C.

We conclude that the results of the magnetization measurements after the annealing process described in Fig. 5(a) can be fully ascribed to particle size effects. To summarize these results, in Fig. 7 we present the RT saturation magnetization M_s and coercive field H_c versus the average particle size D. Evidently, M_s and H_c drop sharply as the average particle size decreases below $\sim$12 nm.[15–17] A fit of the experimental data for H_c to the relation $H_c \propto [1-(D_p/D)^{3/2}]$, defines the critical size $D_p \simeq 8.6$ nm below which the particles become superparamagnetic.[2]

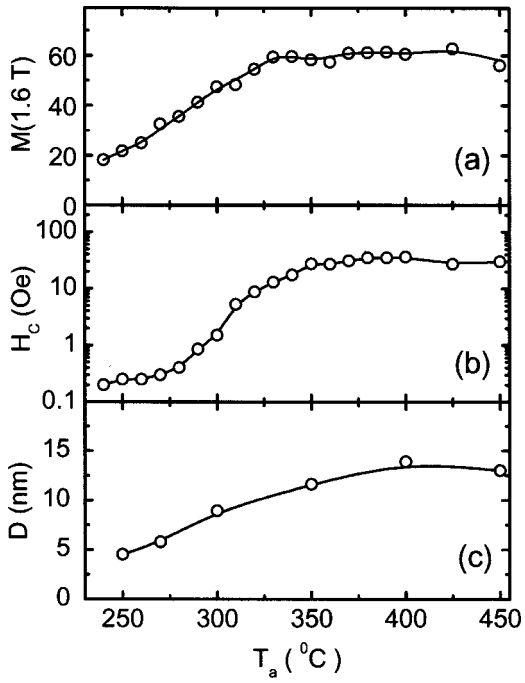

FIG. 6. (a) RT magnetization, (b) coercive field, and (c) average size of γ-Fe_2O_3 particles obtained after annealing at various temperatures.

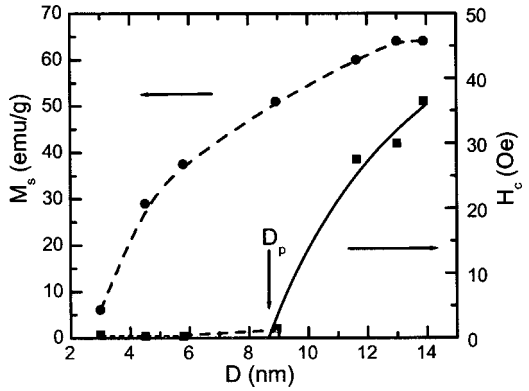

FIG. 7. RT saturation magnetization M_s and coercive field H_c vs average particle size D. Dashed lines are a guide to the eye. Solid line is a fit to $H_c \propto [1-(D_p/D)^{3/2}]$.

V. PHASE TRANSFORMATIONS

As mentioned in the previous section, the growth of the γ-Fe_2O_3 nanocrystals may be accompanied by transformations to other iron–oxide phases.[1,18] Phase transformation to Fe_3O_4 occurring during the initial stages of the growth process was noticed in measurements of the magnetization of as-prepared samples versus temperature in vacuum. Figure 8 shows the magnetization M normalized to the RT magnetization $M_0 = 2.1$ emu/g, measured with an applied magnetic field of 5 kOe in vacuum. Temperature was increased at a rate of 10 °C/min from 27 to 640 °C, and then decreased at a rate dictated by the natural cooling of the furnace. Upon heating, the normalized magnetization $M(T)/M_0$ exhibits a non-monotonic behavior: initially it decreases with temperature up to approximately 200 °C, then it exhibits a sharp increase up to $\sim$400 °C followed by a decrease as the Curie temperature $T_c \approx 570$ °C is approached. This nonmonotonic behavior can be explained as resulting from two competing processes: the normal *decrease* of magnetization with temperature as the Curie point is approached, and the *increase* in the magnetization with temperature due to the increase in the

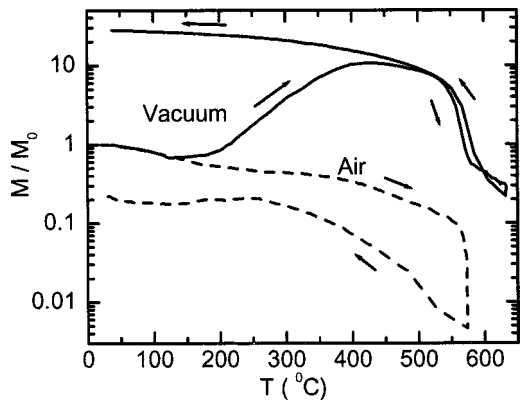

FIG. 8. Normalized magnetization vs temperature for sample in vacuum (solid line) and in air (dashed).

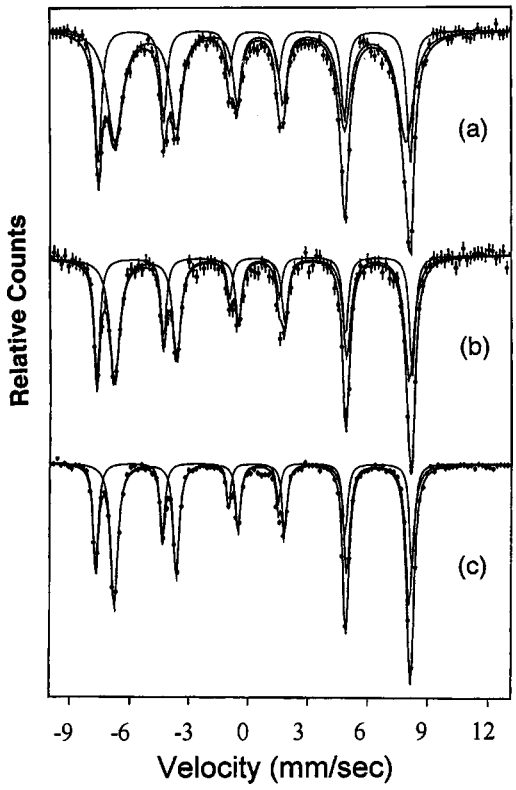

FIG. 9. RT MS of Fe_3O_4 obtained by annealing as prepared Fe_2O_3 at: (a) $T_a=500\,^{\circ}C$ for 8 ks, (b) $T_a=600\,^{\circ}C$ for 12 ks; and (c) commercial Fe_3O_4.

average particle size and magnetic ordering, as discussed in the previous section. Indeed, upon cooling the magnetization exhibits the normal behavior of the magnetically ordered phase, as no particle size changes take place. However, we noticed that during this temperature cycle a phase transformation has also occurred. This was indicated by a change of the sample color from brown to black, and further confirmed by Mössbauer spectroscopy which clearly identified the final phase as Fe_3O_4. MS of such samples are shown in Figs. 9(a) and 9(b) together with the MS of commercial Fe_3O_4 [Fig. 9(c)]. The spectra shown in Figs. 9(a) and 9(b) were measured at room temperature after annealing at $T_a=500\,^{\circ}C$ for 2 h and $T_a=600\,^{\circ}C$ for 3 h, respectively. Comparing these spectra with the spectrum of commercial Fe_3O_4 [Fig. 9(c)], one identifies similar features. Basically, these spectra consist of two superimposed sextets corresponding to two different sites of Fe^{+3} and Fe^{+2} ions. Analysis of the spectrum shown in Fig. 9(a) yields $H_{\mathrm{eff}}=493$ kOe, IS $=0.70(1)$ mm/s, and $H_{\mathrm{eff}}=461$ kOe, IS$=0.17(1)$ mm/s for the two sextets, respectively. These results are in agreement with the hyperfine parameters of commercial Fe_3O_4.[1,19] The Fe_3O_4 phases corresponding to Figs. 8(a) and 8(b) exhibited a RT saturation magnetization of 87 and 93 emu/g, coercive field of 70 and 110 Oe, and average particle size of about 20 and 25 nm, respectively. These magnetization values are higher than those of γ-Fe_2O_3 crystallites of the same size.

A different phase transformation was noticed when the samples were heated in air. The dashed line in Fig. 8 show results of magnetization measurements in air on heating and natural cooling at the same rates as described above. Upon heating, the normalized magnetization decreases monotonically with temperature. On cooling, the magnetization follows a different curve, much lower than the curve obtained during heating. The RT product exhibits a change of color from brown to red–brown, and low normalized magnetization of ~ 0.2, i.e., much smaller than that of the as-prepared material. The TEM image of this product, [Fig. 1(c)] shows a change in the morphology of the particles from spherical to elongated shape with average length of 30 nm and a mean diameter of 18 nm. The decrease in the magnetization despite the increase in the particle size clearly indicates a phase transformation, most likely from γ-Fe_2O_3 to α-Fe_2O_3.

A phase transformation to α-Fe_2O_3 was also noticed by isothermal magnetization in long time annealing experiments in vacuum at temperatures above $450\,^{\circ}C$. The results of these experiments are shown in Fig. 5(b). For $T_a>470\,^{\circ}C$ the magnetization *decreases* after $t_a>3h$. The final product is a red–brown colored α-Fe_2O_3, with relatively small magnetization. Transformation from γ-Fe_2O_3 to α-Fe_2O_3 above $450\,^{\circ}C$ was previously noticed in different types of measurements.[14,18,20]

VI. CONCLUSIONS

Nanophases of γ-Fe_2O_3 with various average particle size can be obtained by annealing of sonochemically synthesized Fe_2O_3 nanoparticles in vacuum at temperatures $240 \leqslant T_a \leqslant 450\,^{\circ}C$ for time periods $2h \lesssim t_a \lesssim 6h$. The growth of the γ-Fe_2O_3 nanocrystallites in vacuum annealing proceeds via the formation of an intermediate Fe_3O_4 phase. γ-Fe_2O_3 crystallites with average size less than 12 nm show magnetic characteristics that strongly differ from those of the bulk γ-Fe_2O_3 phase. Annealing of γ-Fe_2O_3 nanoparticles in air results in a direct transformation into the α-Fe_2O_3 nanophase. An indirect transformation into the α-Fe_2O_3 nanophase via intermediate Fe_3O_4 and γ-Fe_2O_3 phases may also be obtained in vacuum annealing at temperatures higher than $450\,^{\circ}C$.

ACKNOWLEDGMENTS

This research was supported by the Israel Ministry of Science, Culture and Sports through an Infrastructure Grant. X.N.X. thanks the Kort Scholarship and China Scholarship Council for supporting his postdoctoral fellowship. The authors thank Dr. W. P. Huang, Dr. Y. Q. Wang, and Dr. G. S. Peng for TEM measurements.

[1] R. M. Cornell and U. Schwertmann, *The Iron Oxides* (VCH Verlagsgesellschaft mbH, Weinheim, Germany, 1996).
[2] B. D. Cullity, *Introduction to Magnetic Materials* (Addison-Wesley, Reading, MA, 1972).
[3] J. M. D. Coey, Phys. Rev. Lett. **25**, 1140 (1971).
[4] S. Mørup and E. Tronc, Phys. Rev. Lett. **72**, 3278 (1994); S. Mørup, Europhys. Lett. **28**, 671 (1994).
[5] B. Martinez, X. Obradors, L. Balcells, A. Rouanet, and C. Monty, Phys. Rev. Lett. **80**, 181 (1998).
[6] F. Bødker, M. F. Hansen, C. Bender Koch, K. Lefmann, and St. Mørup, Phys. Rev. B **61**, 6826 (2000).
[7] M. E. McHenry, M. A. Willard, and D. E. Laughlin, Prog. Mater. Sci. **44**, 241 (1999).
[8] D. L. Leslie-Pelecky and R. D. Rieke, Chem. Mater. **8**, 1770 (1996).
[9] M. P. Sharrock and R. E. Bodnar, J. Appl. Phys. **57**, 3919 (1985).

[10] M. R. Anantharaman, K. V. Joseph, and H. V. Keer, Bull. Mater. Sci. **20**, 975 (1997).
[11] F. Albert Cotton and G. Wilkinson, *Advanced Inorganic Chemistry—A Comprehensive Text* (Interscience, New York, 1962), p. 700.
[12] X. Cao, Yu. Koltypin, R. Prozorov, G. Kataby, and A. Gedanken, J. Mater. Chem. **7**, 2447 (1997); X. Cao, R. Prozorov, Yu. Koltypin, G. Kataby, I. Felner, and A. Gedanken, J. Mater. Res. **12**, 402 (1997).
[13] T. Prozorov, R. Prozorov, Yu. Koltypin, I. Felner, and A. Gedanken, J. Phys. Chem. B **102**, 10165 (1998).
[14] R. Keller and E. Schmidbauer, J. Magn. Magn. Mater. **162**, 85 (1996).
[15] G. Herzer, Scr. Metall. Mater. **33**, 1741 (1995).
[16] G. Herzer, IEEE Trans. Magn. **26**, 1397 (1990).
[17] D. H. Han, J. P. Wang, and H. L. Luo, J. Magn. Magn. Mater. **136**, 176 (1994).
[18] E. Trone, J. P. Jolivet, and J. Livage, Hyperfine Interact. **54**, 737 (1990).
[19] A. Hartridge, A. K. Bhattacharya, M. Sengupta, C. K. Majumdar, D. Das, and S. N. Chintalapudi, J. Magn. Magn. Mater. **176**, L89 (1997).
[20] D. Prodan, C. Chanéac, E. Tronc, J. P. Jolivet, R. Cherkaour, A. Ezzir, M. Nogués, and J. L. Mormann, J. Magn. Magn. Mater. **203**, 63 (1999).